

Regular Time-series Generation using SGM*

Haksoo Lim¹, Minjung Kim², Sewon Park², Noseong Park¹

¹Yonsei University, ²Samsung SDS
limhaksoo96@yonsei.ac.kr, mj100.kim@samsung.com,
sw0413.park@samsung.com, noseong@yonsei.ac.kr

Abstract

Score-based generative models (SGMs) are generative models that are in the spotlight these days. Time-series frequently occurs in our daily life, e.g., stock data, climate data, and so on. Especially, time-series forecasting and classification are popular research topics in the field of machine learning. SGMs are also known for outperforming other generative models. As a result, we apply SGMs to synthesize time-series data by learning conditional score functions. We propose a conditional score network for the time-series generation domain. Furthermore, we also derive the loss function between the score matching and the denoising score matching in the time-series generation domain. Finally, we achieve state-of-the-art results on real-world datasets in terms of sampling diversity and quality.

Introduction

SGMs now show remarkable results throughout various fields, including image generation, voice synthesis, etc. (Ahmed et al. 2010; Fu 2011; Ismail Fawaz et al. 2019). Let $\{(\mathbf{x}_i, t_i)\}_{i=1}^N$ be a time-series sample which consists of N observations. In many cases, however, time-series samples are incomplete and/or the number of samples is insufficient, in which case training machine learning models cannot be fulfilled in a robust way. To overcome the limitation, time-series synthesis has been studied actively recently. These synthesis models have designed in various ways, including variational autoencoder (VAE) and generative adversarial network (GAN) (Desai et al. 2021; Yoon, Jarrett, and van der Schaar 2019).

In the image generation field, score-based generative models (SGMs) (or diffusion models) have recently attracted much attention for their superior sampling quality and diversity over other generative paradigms (Song et al. 2021; Xiao, Kreis, and Vahdat 2022). Being inspired by their results, many researchers attempted to apply SGMs to other generation tasks, such as medical image processing and voice synthesis (Mittal et al. 2021; Song et al. 2022), etc.

Although there exist several efforts to generate time-series, according to our survey, there is no research using SGMs

Method	Domain	Type	Target score function
TimeGrad	Forecasting	Diffusion	$\nabla \log p(\mathbf{x}_t^s \mathbf{h}_{t-1})$
ScoreGrad	Forecasting	Energy	$\nabla \log p(\mathbf{x}_t^s \mathbf{x}_t)$
CSDI	Imputation	Diffusion	$\nabla \log p(\mathbf{x}_{t_q}^s \mathbf{x}_{co})$
TSGM (Ours)	Generation	SGM	$\nabla \log p(\mathbf{h}_t^s \mathbf{h}_t)$

Table 1: Qualitative comparison among score-based methods for time-series

— there exist time-series SGMs only for forecasting and imputation (Rasul et al. 2021; Yan et al. 2021; Tashiro et al. 2021) (cf. Table 1). Therefore, we extend SGMs into the field of time-series synthesis. Our time-series synthesis is technically different from time-series forecasting, which forecast future observations given past observations, and time-series imputation, which given a time-series sample with missing observations, fills out those missing observations. We discuss about the differences in the related work section in detail. Unlike the image generation which generates each image independently, in addition, time-series generation must generate each observation considering its past generated observations, i.e., conditional sampling. To this end, in this paper, we propose the method of time-series generation using conditional score-based generative model (TSGM).

We design the first conditional score network on time-series generation, which learns the gradient of the conditional log-likelihood with respect to time. We also design a denoising score matching on time-series generation — existing SGM-based time-series forecasting and imputation methods also have their own denoising score matching definitions, but our denoising score matching differs from theirs due to the task difference (cf. Table 1). Our TSGM can be further categorized into two types depending on the used stochastic differential equation type: VP, and subVP.

We conduct in-depth experiments with 5 real-world datasets and 2 key evaluation metrics — therefore, there are, in total, 10 different evaluation cases. Our specific choice of 8 baselines includes almost all existing types of time-series generative paradigms, ranging from VAEs to GANs. Our proposed method shows the best generation quality in all but two cases. We also visualize real and generated time-series samples onto a latent space using t-SNE (van der Maaten and Hinton 2008) and those visualization results intuitively show that our method’s generation diversity is also the best

*This paper is under review.

among those baselines. Our contributions can be summarized as follows:

1. We, for the first time, propose a SGM-based time-series synthesis method (although there exist SGM-based time-series forecasting and imputation methods).
2. We derive our own denoising score matching mechanism which is different other existing ones, considering the fully recurrent nature of our time-series generation.
3. We conduct comprehensive experiments with 5 real-world datasets and 8 baselines. Overall, our proposed method shows the best generation quality and diversity.

Related Work and Preliminaries

We review the literature for SGMs and time-series generation, followed by preliminary knowledge.

Score-based Generative Models

SGMs are one of the most popular image generation methods. It has several advantages over other generative models for its generation quality, computing exact log-likelihood, and controllable generation without extra training. For its remarkable results, lots of researchers try to apply them to other fields, e.g., voice synthesis (Mittal et al. 2021), medical image process (Song et al. 2022), etc. SGMs consists of the following two procedures: i) they first add Gaussian noises into a sample, ii) and then remove the added noises to recover new sample. Those two processes are called as forward and reverse process, respectively.

Forward Process At first, SGMs add noises with the following stochastic differential equation (SDE):

$$d\mathbf{x}^s = \mathbf{f}(s, \mathbf{x}^s)ds + g(s)d\mathbf{w}, \quad s \in [0, 1], \quad (1)$$

where $\mathbf{w} \in \mathbb{R}^n$ is n dimensional Brownian motion, $\mathbf{f}(s, \cdot) : \mathbb{R}^n \rightarrow \mathbb{R}^n$ is vector-valued drift term, and $g : [0, 1] \rightarrow \mathbb{R}$ is scalar-valued diffusion functions. Here after, we define \mathbf{x}^s as a noisy sample diffused at time $s \in [0, 1]$ from an original sample $\mathbf{x} \in \mathbb{R}^n$. Therefore, \mathbf{x}^s can be understood as a stochastic process following the SDE. There are several options for \mathbf{f} and g : variance exploding (VE), variance preserving (VP), and subVP. (Song et al. 2021) proved that VE and VP are continuous generalizations of the two discrete diffusion methods, (Sohl-Dickstein et al. 2015; Ho, Jain, and Abbeel 2020) and (Song and Ermon 2019). In addition, the author further suggested the subVP method, which is a modified version of VP.

SGMs run the forward SDE with sufficiently large N steps to make it sure that the diffused sample converges to a Gaussian distribution at the final step. The score network $M_\theta(s, \mathbf{x}^s)$ learns the gradient of the log-likelihood $\nabla_{\mathbf{x}^s} \log p(\mathbf{x}^s)$, which will be used in the reverse process.

Reverse Process For each forward SDE from $s = 0$ to 1, (Anderson 1982) proved that there exists the following corresponding reverse SDE:

$$d\mathbf{x}^s = [\mathbf{f}(s, \mathbf{x}^s) - g^2(s)\nabla_{\mathbf{x}^s} \log p(\mathbf{x}^s)]ds + g(s)d\bar{\mathbf{w}}.$$

The formula suggests that if knowing the score function, $\nabla_{\mathbf{x}^s} \log p(\mathbf{x}^s)$, we can recover real samples from the prior

distribution $p_1(\mathbf{x}) \sim \mathcal{N}(\mu, \sigma^2)$, where μ, σ vary depending on the forward SDE type.

Training and Sampling In order for the model M to learn the score function, the model has to optimize the following loss function:

$$L(\theta) = \mathbb{E}_s \{ \lambda(s) \mathbb{E}_{\mathbf{x}^s} [\|M_\theta(s, \mathbf{x}^s) - \nabla_{\mathbf{x}^s} \log p(\mathbf{x}^s)\|_2^2] \},$$

where s is uniformly sampled over $[0, 1]$ with an appropriate weight function $\lambda(s) : [0, 1] \rightarrow \mathbb{R}$. However, using the above formula is problematic since we do not know the exact gradient of the log-likelihood. Thanks to (Vincent 2011), the loss can be substituted with the following denoising score matching loss:

$$L^*(\theta) = \mathbb{E}_s \{ \lambda(s) \mathbb{E}_{\mathbf{x}^0} \mathbb{E}_{\mathbf{x}^s | \mathbf{x}^0} [\|M_\theta(s, \mathbf{x}^s) - \nabla_{\mathbf{x}^s} \log p(\mathbf{x}^s | \mathbf{x}^0)\|_2^2] \}.$$

Since SGMs use an affine drift term, the transition kernel $p(\mathbf{x}^s | \mathbf{x}^0)$ follows a certain Gaussian distribution (Särkkä and Solin 2019) and therefore, $\nabla_{\mathbf{x}^s} \log p(\mathbf{x}^s | \mathbf{x}^0)$ can be analytically calculated.

Time-series Generation and SGMs

Time-series Generation In order to synthesize time-series $\mathbf{x}_{1:T}$, unlike other generation tasks, we must generate each observation \mathbf{x}_t at time $t \in [2 : T]$ considering its previous history $\mathbf{x}_{1:t-1}$. One can train neural networks to learn the conditional likelihood $p(\mathbf{x}_t | \mathbf{x}_{1:t-1})$ and generate each \mathbf{x}_t recursively using it. There are several time-series generation papers, and we introduce their ideas.

TimeVAE (Desai et al. 2021) is a variational autoencoder to synthesize time-series data. This model can provide interpretable results by reflecting temporal structures such as trend and seasonality in the generation process. TimeGAN (Yoon, Jarrett, and van der Schaar 2019) uses a GAN architecture to generate time-series. First, it trains an encoder and decoder, which transform a time-series sample $\mathbf{x}_{1:T}$ into latent vectors $\mathbf{h}_{1:T}$ and recover them by using a recurrent neural network (RNN). Next, it trains a generator and discriminator pair on latent space, by minimizing discrepancy between ground-truth $p(\mathbf{x}_t | \mathbf{x}_{1:t-1})$ and synthesized $\hat{p}(\mathbf{x}_t | \mathbf{x}_{1:t-1})$. Since it uses an RNN-based encoder, it can efficiently learn the conditional likelihood $p(\mathbf{x}_t | \mathbf{x}_{1:t-1})$ by treating it as $p(\mathbf{h}_t | \mathbf{h}_{t-1})$, since $\mathbf{h}_t \sim \mathbf{x}_{1:t}$ under the regime of RNNs. Therefore, it can generate each observation \mathbf{x}_t considering its previous history $\mathbf{x}_{1:t-1}$. However, GAN-based generative models are vulnerable to the issue of mode collapse (Xiao, Kreis, and Vahdat 2022) and unstable behavior problems during training (Chu, Minami, and Fukumizu 2020). There also exist GAN-based methods to generate other types of sequential data, e.g., video, sound, etc (Esteban, Hyland, and Rätsch 2017; Mogren 2016; Xu et al. 2020; Donahue, McAuley, and Puckette 2019). In our experiments, we also use them as our baselines for thoroughly evaluating our method.

SGMs on Time-series Although there exist a little research work using their own conditional score networks, TimeGrad (Rasul et al. 2021) and ScoreGrad (Yan et al. 2021) are for time-series forecasting, and CSDI (Tashiro et al. 2021) is for time-series imputation.

In TimeGrad (Rasul et al. 2021), the authors used a diffusion model, which is a discrete version of SGMs, to forecasting future observations given past observations by minimizing the following objective function:

$$\sum_{t=t_0}^T -\log p_{\theta}(\mathbf{x}_t | \mathbf{x}_{1:t-1}, \mathbf{c}_{1:T}),$$

where $\mathbf{c}_{1:T}$ means the covariates of $\mathbf{x}_{1:T}$. The above formula assume that we already know $\mathbf{x}_{1:t_0-1}$, and by using an RNN encoder, $(\mathbf{x}_{1:t}, \mathbf{c}_{1:T})$ can be encoded into \mathbf{h}_t . After training, the model forecasts future observations recursively. After taking $\mathbf{x}_{1:t}$, it encodes with $\mathbf{c}_{1:T}$ into \mathbf{h}_t , and forecast the next step observation \mathbf{x}_{t+1} from the previous condition \mathbf{h}_t .

In the perspective of SGMs, TimeGrad and ScoreGrad can be regarded as methods to train the following conditional score network M :

$$\sum_{t=t_0}^T \mathbb{E}_s \mathbb{E}_{\mathbf{x}_t^s} \|M_{\theta}(s, \mathbf{x}_t^s, \mathbf{h}_{t-1}) - \nabla_{\mathbf{x}_t^s} \log p(\mathbf{x}_t^s | \mathbf{h}_{t-1})\|_2^2.$$

We denote \mathbf{x}_t^s as \mathbf{x}_t at step s . Note that s is uniformly sampled from $[0, 1]$ as in (Song et al. 2021).

(Yan et al. 2021) proposed an energy-based generative method for forecasting. Almost all notations and ideas are the same as those in (Rasul et al. 2021), except that it generalizes diffusion models into the energy-based field. The used training loss is as follows:

$$\sum_{t=t_0}^T \mathbb{E}_s \mathbb{E}_{\mathbf{x}_t} \mathbb{E}_{\mathbf{x}_t^s | \mathbf{x}_t} \|M_{\theta}(s, \mathbf{x}_t^s, \mathbf{x}_{1:t-1}) - \nabla_{\mathbf{x}_t^s} \log p(\mathbf{x}_t^s | \mathbf{x}_t)\|_2^2.$$

By using a continuous model, (Yan et al. 2021) achieved good results outperforming (Rasul et al. 2021). (Tashiro et al. 2021) proposed a general diffusion framework which can be applied to various domains, including not only imputation, but also forecasting and interpolations. CSDI reconstructs an entire sequence at once, not recursively. Although the model takes a diffusion framework, their loss can be written as follows:

$$\mathbb{E}_s \mathbb{E}_{\mathbf{x}_{ta}^s} \|M_{\theta}(s, \mathbf{x}_{ta}^s, \mathbf{x}_{co}) - \nabla \log p(\mathbf{x}_{ta}^s | \mathbf{x}_{co})\|_2^2,$$

where \mathbf{x}_{co} and \mathbf{x}_{ta} are conditions and imputation targets, respectively. By training a score network using the above loss, the model generates an entire sequence from a partial sequence.

Although (Rasul et al. 2021; Yan et al. 2021) earned the state-of-the-art results for forecasting and imputation, we found that they are not suitable for our generative task due to the fundamental mismatch between their score function definitions and our task (cf. Table 1). For instance, TimeGrad generates future observations given the hidden representation of past observations \mathbf{h}_{t-1} , i.e., a representative forecasting structure.

As a remedy, we propose to optimize a conditional score network by using the following denoising score matching:

$$\mathbb{E}_s \mathbb{E}_{\mathbf{h}_{1:T}} \sum_{t=1}^T \|M_{\theta}(s, \mathbf{h}_t^s, \mathbf{h}_{t-1}) - \nabla_{\mathbf{h}_t^s} \log p(\mathbf{h}_t^s | \mathbf{h}_t)\|_2^2.$$

We denote $\mathbf{h}_0 = \mathbf{0}$. Unlike other models (Rasul et al. 2021; Yan et al. 2021; Tashiro et al. 2021) which resort to existing known proofs, we prove the correctness of our denoising score matching loss in Theorem (1).

Proposed Methods : TSGM

TSGM consists of three networks: an encoder, a decoder, and a conditional score network. Firstly, we train the encoder and the decoder to embed time-series into a latent space. Next, using the pre-trained encoder and decoder, we train the conditional score network. The conditional score network will be used for sampling fake time-series.

Encoder and Decoder

The encoder and decoder map time-series to a latent space and vice versa. Let \mathcal{X} and \mathcal{H} denote a data space and a latent space. Next, e and d are an embedding function mapping \mathcal{X} to \mathcal{H} and vice versa. We define $\mathbf{x}_{1:T}$ as time-series sample with a length of T , and \mathbf{x}_t is a multi-dimensional observation in $\mathbf{x}_{1:T}$ at time t . Similarly, $\mathbf{h}_{1:T}$ and \mathbf{h}_t are embedded vectors. The encoder e and decoder d are constructed using recurrent neural networks. Since TSGM uses RNNs, both e and d are defined recursively as follows:

$$\mathbf{h}_t = e(\mathbf{h}_{t-1}, \mathbf{x}_t), \quad \hat{\mathbf{x}}_t = d(\mathbf{h}_t), \quad (2)$$

where $\hat{\mathbf{x}}_t$ denotes a reconstructed time-series sample at time t . After embedding real time-series data onto a latent space, we can train the conditional score network with its conditional log likelihood, which will be described in the following subsection. The encoder and decoder are pre-trained before our main training with the proposed denoising score matching.

Conditional Score Network

Unlike other generation tasks, e.g., image generation (Song et al. 2021), tabular data synthesis (Kim et al. 2022), where each sample is independent, time-series observations are dependent to previous observations. Therefore, the score network for time-series generation must be designed to learn the conditional log likelihood on previous generated observations, which is more complicated than that in image generation.

In order to learn the conditional log likelihood, we modify the popular U-net (Ronneberger, Fischer, and Brox 2015) architecture for our purpose. Since U-net has achieved various good results for previous generative tasks (Song and Ermon 2019; Song et al. 2021), we modify its 2-dimensional convolution layers to 1-dimensional ones for handling time-series observations. Then we concatenate diffused data with condition, and use the concatenated one and temporal feature as input to learn score function. More details are in the training and sampling procedures section.

Training Objective Functions

We use two training objective functions. First, we train the encoder and the decoder using L_{ed} . Let $\mathbf{x}_{1:T} \sim p(\mathbf{x}_{1:T})$ and $\hat{\mathbf{x}}_{1:T}$ denote an input time-series sample and its reconstructed copy by the encoder-decoder process, respectively. Then,

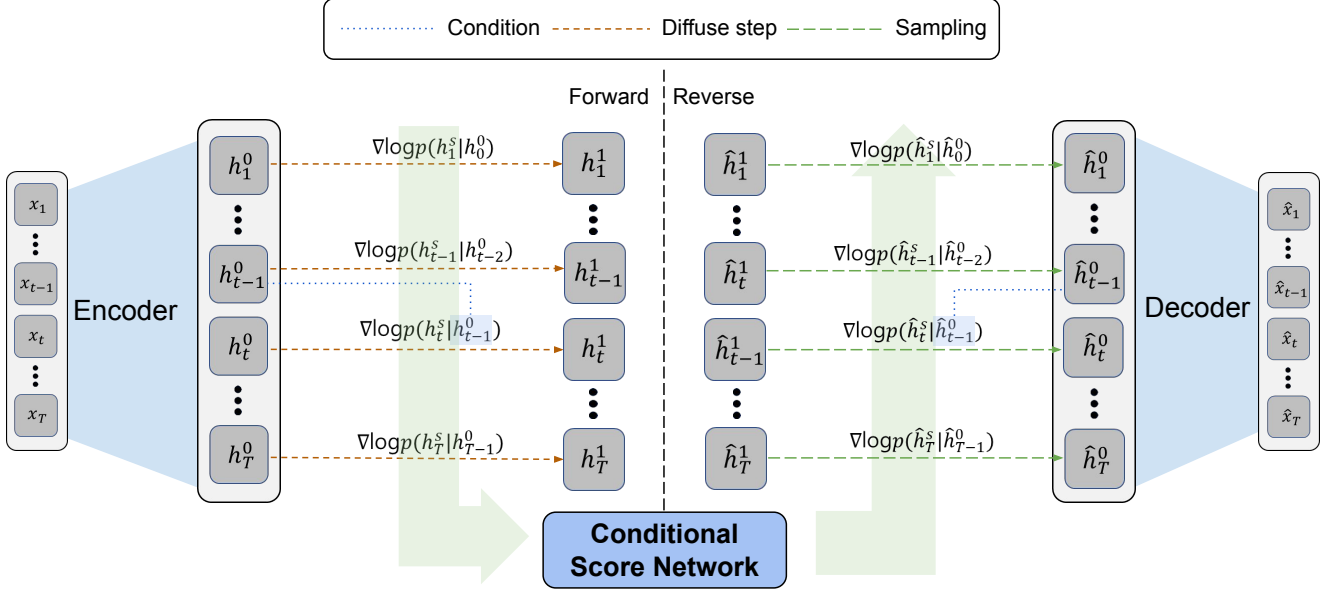


Figure 1: The overall workflow of TSGM

L_{ed} means the following MSE loss between $\mathbf{x}_{1:T}$ and its reconstructed copy $\hat{\mathbf{x}}_{1:T}$:

$$L_{ed} = \mathbb{E}_{\mathbf{x}_{1:T}} [\|\hat{\mathbf{x}}_{1:T} - \mathbf{x}_{1:T}\|_2^2]. \quad (3)$$

Next, we define another loss L_{score} to train the conditional score network, which is one of our main contributions. At time t in $[1 : T]$, we diffuse $\mathbf{x}_{1:t}$ through a sufficiently large number of steps of the forward SDE to a Gaussian distribution. Let $\mathbf{x}_{1:t}^s$ denotes a diffused sample at step $s \in [0, 1]$ from $\mathbf{x}_{1:t}$. Then, the conditional score network $M_\theta(s, \mathbf{x}_{1:t}^s, \mathbf{x}_{1:t-1})$ learns the gradient of the conditional log-likelihood with following L_1 :

$$L_1 = \mathbb{E}_s \mathbb{E}_{\mathbf{x}_{1:T}} \left[\sum_{t=1}^T \lambda(s) l_1(t, s) \right], \quad (4)$$

where

$$l_1(t, s) = \mathbb{E}_{\mathbf{x}_{1:t}^s} \left[\left\| M_\theta(s, \mathbf{x}_{1:t}^s, \mathbf{x}_{1:t-1}) - \nabla_{\mathbf{x}_{1:t}^s} \log p(\mathbf{x}_{1:t}^s | \mathbf{x}_{1:t-1}) \right\|_2^2 \right]$$

that $\nabla_{\mathbf{x}_{1:t}^s} \log p(\mathbf{x}_{1:t}^s | \mathbf{x}_{1:t-1})$, where \mathbf{x}_i in depends on $\mathbf{x}_{1:i-1}$ for each $i \in [2, t]$, is designed specially for time-series generation. Note that for our training, $\mathbf{x}_{1:t}^s$ is sampled from $p(\mathbf{x}_{1:t}^s | \mathbf{x}_{1:t-1})$ and s is uniformly sampled from $[0, 1]$. Thanks to following theorem, we can use the efficient denoising score loss L_2 to train the conditional score network. We set $\mathbf{x}_0 = \mathbf{0}$.

Theorem 1 (Denoising score matching on time-series). $l_1(t, s)$ can be replaced by the following $l_2(t, s)$:

$$l_2(t, s) = \mathbb{E}_{\mathbf{x}_t} \mathbb{E}_{\mathbf{x}_{1:t}^s} \left[\left\| M_\theta(s, \mathbf{x}_{1:t}^s, \mathbf{x}_{1:t-1}) - \nabla_{\mathbf{x}_{1:t}^s} \log p(\mathbf{x}_{1:t}^s | \mathbf{x}_{1:t-1}) \right\|_2^2 \right],$$

where \mathbf{x}_t and $\mathbf{x}_{1:t}^s$ are sampled from $p(\mathbf{x}_t | \mathbf{x}_{1:t-1})$ and $p(\mathbf{x}_{1:t}^s | \mathbf{x}_{1:t-1})$. Therefore, we can use an alternative objective,

$$L_2 = \mathbb{E}_s \mathbb{E}_{\mathbf{x}_{1:T}} \left[\sum_{t=1}^T \lambda(s) l_2(t, s) \right] \text{ instead of } L_1$$

Proof. We first decompose $l_1(t, s)$ into three parts. We then transform each part by inducing the following result: $\mathbb{E}_{\mathbf{x}_{1:t}^s} \nabla_{\mathbf{x}_{1:t}^s} \log p(\mathbf{x}_{1:t}^s | \mathbf{x}_{1:t-1}) = \mathbb{E}_{\mathbf{x}_t} \mathbb{E}_{\mathbf{x}_{1:t}^s} \nabla_{\mathbf{x}_{1:t}^s} \log p(\mathbf{x}_{1:t}^s | \mathbf{x}_{1:t-1})$. Detailed proof is in Appendix. \square

Next, we describe another corollary to formulate our loss.

Corollary 1. Our target objective function, L_{score} , is defined as follows:

$$L_{score} = \mathbb{E}_s \mathbb{E}_{\mathbf{x}_{1:T}} \left[\sum_{t=1}^T \lambda(s) l_2^*(t, s) \right],$$

where

$$l_2^*(t, s) = \mathbb{E}_{\mathbf{x}_{1:t}^s} \left[\left\| M_\theta(s, \mathbf{x}_{1:t}^s, \mathbf{x}_{1:t-1}) - \nabla_{\mathbf{x}_{1:t}^s} \log p(\mathbf{x}_{1:t}^s | \mathbf{x}_{1:t-1}) \right\|_2^2 \right].$$

Then, $L_2 = L_{score}$ is satisfied.

The proof of Corollary 1 is given in Appendix. Note that the loss L_2 cannot be used in practice since it has to sample each \mathbf{x}_t using $p(\mathbf{x}_t | \mathbf{x}_{1:t-1})$ every time. So we use the loss L_{score} for our training.

Since we pre-train the encoder and decoder, the encoder can embeds $\mathbf{x}_{1:t}$ into $\mathbf{h}_t \in \mathcal{H}$. Ideally, \mathbf{h}_t involves the entire information of $\mathbf{x}_{1:t}$, but we want to consider more practical cases. Thus, we define \mathcal{H} as a latent space having the past information by setting up window size K as constant sequential length of each sample (details are in the experimental setup section). Therefore, L_{score} can be re-written as follows with the embedding into the latent space:

$$L_{score}^{\mathcal{H}} = \mathbb{E}_s \mathbb{E}_{\mathbf{h}_{1:T}} \sum_{t=1}^T [\lambda(s) l_3(t, s)], \quad (5)$$

with $l_3(t, s) = \mathbb{E}_{\mathbf{h}_t^s} \left[\left\| M_\theta(s, \mathbf{h}_t^s, \mathbf{h}_{t-1}) - \nabla_{\mathbf{h}_t^s} \log p(\mathbf{h}_t^s | \mathbf{h}_t) \right\|_2^2 \right]$. $L_{score}^{\mathcal{H}}$ is what we use for our experiments (instead of L_{score}). Until now, we introduced our target objective functions, L_{ed} and $L_{score}^{\mathcal{H}}$. We note that we use the exactly same weight $\lambda(s)$ as that in (Song et al. 2021).

Algorithm 1: Training algorithm

Input: $\mathbf{x}_{1:T}$

Parameter:

use_{alt} = A Boolean parameter to set whether to use the alternating training method.

$iter_{pre}$ = The number of iterations for pre-training

$iter_{main}$ = The number of iterations for training

Output: $Encoder, Decoder, M_\theta$

```

1: for  $iter \in \{1, \dots, iter_{pre}\}$  do
2:   Train  $Encoder$  and  $Decoder$  by using  $L_{ed}$ 
3: end for
4: for  $iter \in \{1, \dots, iter_{main}\}$  do
5:   Train  $M_\theta$  by using  $L_{score}^{\mathcal{H}}$ 
6:   if  $use_{alt}$  then
7:     Train the  $Encoder$  and  $Decoder$  by using  $L_{ed}$ 
8:   end if
9: end for
10: return  $Encoder, Decoder, M_\theta$ 

```

Training and Sampling Procedures

We explain the details about its training method with an intuitive example in Fig. 1. At first, we pre-train both the encoder and decoder using L_{ed} . After pre-training them, we train the conditional score network. When training the conditional score network, we use the embedded hidden vectors produced by the encoder. After encoding an input $\mathbf{x}_{1:T}$, we obtain its latent vectors $\mathbf{h}_{1:T}$ — we note that each hidden vector \mathbf{h}_t has all the previous information on or before t since the encoder is an RNN-based encoder. We use the following forward process (Song et al. 2021), where t means the physical time of the input time-series in $[1 : T]$ and s denotes the time of the diffusion step :

$$d\mathbf{h}_t^s = \mathbf{f}(s, \mathbf{h}_t^s)ds + g(s)d\mathbf{w}, \quad s \in [0, 1].$$

During the forward process, the conditional score network reads the pair $(s, \mathbf{h}_t^s, \mathbf{h}_{t-1})$ as input and thereby, it can learn the conditional score function $\nabla \log p(\mathbf{h}_t^s | \mathbf{h}_{t-1})$ by using $L_{score}^{\mathcal{H}}$, where $\mathbf{h}_0 = \mathbf{0}$. We train the conditional score network and the encoder-decoder pair alternately after the pre-training step. For some datasets, we found that train only the conditional score network achieve better results after pre-training the autoencoder. Therefore, $use_{alt} = \{True, False\}$ is a hyperparameter to set whether we use the alternating training method. We give the detailed training procedure in Algorithm 1

After the training procedure, we use the following conditional reverse process:

$$d\mathbf{h}_t^s = [\mathbf{f}(s, \mathbf{h}_t^s) - g^2(s)\nabla_{\mathbf{h}_t^s} \log p(\mathbf{h}_t^s | \mathbf{h}_{t-1})]ds + g(s)d\bar{\mathbf{w}},$$

where s is uniformly sampled over $[0, 1]$. The conditional score function in this process can be replaced with the trained score network $M_\theta(s, \mathbf{h}_t^s, \mathbf{h}_{t-1})$. The detailed sampling method is as follows:

- At first, we sample \mathbf{z}_0 from a Gaussian prior distribution and concatenate it with \mathbf{h}_0 . We consider the concatenated vector and temporal feature as inputs to the

conditional score network and generates initial data $\hat{\mathbf{h}}_1$ with the *predictor-corrector* method (Song et al. 2021).

- We repeat the following computation for every $1 < t \leq T$, i.e., recursive generation. After reading the previously generated samples $\hat{\mathbf{h}}_{t-1}$ for $t \in [2, T]$, we sample \mathbf{z}_{t-1} from a Gaussian prior distribution and concatenate it with $\hat{\mathbf{h}}_{t-1}$. We use it and temporal feature, s , as inputs to the conditional score network $M_\theta(s, \mathbf{h}_t^s, \mathbf{h}_{t-1})$ and synthesize the next latent vector $\hat{\mathbf{h}}_t$ via the *predictor-corrector* step.

Once the sampling procedure is finished, we can reconstruct $\hat{\mathbf{x}}_{1:T}$ from $\hat{\mathbf{h}}_{1:T}$ using the trained decoder at once.

Experiments

We describe our detailed experimental environments and results.

Experimental Environments

We use 5 real-world datasets from various fields with 8 baselines. We refer to Appendix for the detailed descriptions on our datasets, baselines, and other software/hardware environments. In particular, our collection of baselines covers almost all existing types of time series synthesis methods, ranging from RNNs to VAEs and GANs. For the baselines, we reuse their released source codes in their official repositories and rely on their designed training and model selection procedures.

Hyperparameters Table 2 shows the best hyperparameters. We define hidden dimension of inputs and temporal features as d_{in} and d_t , respectively. For other settings, we use the default values in TimeGAN (Yoon, Jarrett, and van der Schaar 2019) and VPSDE (Song et al. 2021). We give the detailed search method in Appendix.

Dataset	d_{in}	d_t	use_{alt}	$iter_{pre}$	$iter_{main}$
Stocks	24	96	True	50000	40000
Energy	56	56	False	100000	
Air	40	80	True	50000	
AI4I	24	96	True	50000	
Occupancy	40	80	False	100000	

Table 2: The best hyperparameters for our method

Evaluation Metrics In the image generation domain, researchers have evaluated the *fidelity* and the *diversity* of models by using the Fréchet inception distance (FID) and inception score (IS). On the other hand, to measure the fidelity and the diversity of synthesized time-series samples, we use the following predictive score and the discriminative score as in (Yoon, Jarrett, and van der Schaar 2019). We strictly follow the agreed evaluation protocol of (Yoon, Jarrett, and van der Schaar 2019) by the time-series research community. Both metrics are designed in a way that lower values are preferred. We run each generative method 10 times with different seeds, and report its mean and standard deviation of the following discriminative and predictive scores:

	Dataset	Stocks	Energy	Air	AI4I	Occupancy
Disc. score	TSGM-VP	.022±.005	.221±.025	.122±.014	.147±.005	.402±.004
	TSGM-subVP	.021±.008	.198±.025	.127±.010	.150±.010	.414±.008
	T-Forcing	.226±.035	.483±.004	.404±.020	.435±.025	.333±.005
	P-Forcing	.257±.026	.412±.006	.484±.007	.443±.026	.411±.013
	TimeGAN	.102±.031	.236±.012	.447±.017	.070±.009	.365±.014
	RCGAN	.196±.027	.336±.017	.459±.104	.234±.015	.485±.001
	C-RNN-GAN	.399±.028	.499±.001	.499±.000	.499±.001	.467±.009
	TimeVAE	.175±.031	.498±.006	.381±.037	.446±.024	.415±.050
	WaveGAN	.217±.022	.363±.012	.491±.013	.481±.034	.309±.039
	COT-GAN	.285±.030	.498±.000	.423±.001	.411±.018	.443±.014
Pred. score	TSGM-VP	.037±.000	.257±.000	.005±.000	.218±.000	.022±.001
	TSGM-subVP	.037±.000	.252±.000	.005±.000	.217±.000	.022±.001
	T-Forcing	.038±.001	.315±.005	.008±.000	.242±.001	.029±.001
	P-Forcing	.043±.001	.303±.006	.021±.000	.220±.000	.070±.105
	TimeGAN	.038±.001	.273±.004	.017±.004	.253±.002	.057±.001
	RCGAN	.040±.001	.292±.005	.043±.000	.224±.001	.471±.002
	C-RNN-GAN	.038±.000	.483±.005	.111±.000	.340±.006	.242±.001
	TimeVAE	.042±.002	.268±.004	.013±.002	.233±.010	.035±.002
	WaveGAN	.041±.001	.307±.007	.009±.000	.225±.006	.034±.008
	COT-GAN	.044±.000	.260±.000	.024±.001	.220±.000	.084±.001
	Original	.036±.001	.250±.003	.004±.000	.217±.000	.019±.000

Table 3: Experimental results in terms of the discriminative and predictive scores. The best scores are in boldface. The statistical significance ($p < 0.05$) of the best results are confirmed in all cases by using the Wilcoxon rank sum test..

i) *Predictive Score*: We use the predictive score to evaluate whether a generative model can successfully reproduce the temporal properties of the original data. To do this, we first train a naive LSTM-based sequence model for time-series forecasting with synthesized samples. The performance of this predictive model is measured as the mean absolute error (MAE) on the original test data. This kind of evaluation paradigm is called as train-synthesized-test-real (TSTR) in the literature.

ii) *Discriminative Score*: In order to assess how similar the original and generated samples are, we train a 2-layer LSTM model that classifies the real/fake samples into two classes, real or fake. We use the performance of the trained classifier on the test data as the discriminative score. Therefore, lower discriminator scores mean that real and fake samples are similar.

Experimental Results

Table 3 shows that achieves remarkable results, outperforming TimeGAN, a state-of-the-art method, except for only two cases: the discriminative scores on AI4I and Occupancy. Especially, for Stock, Energy, and Air, TSGM exhibits overwhelming performance by large margins for the discriminative score. Moreover, for the predictive score, TSGM performs best and obtains almost the same scores with that of the original data, which indicates that generated samples from TSGM preserve almost all the predictive characteristics of the original data.

We also show t-SNE visualizations in Figure 2. TimeGAN and TimeVAE are two representative VAE and GAN-based baselines, respectively. In the figure, the synthetic samples generated from TSGM consistently show successful

	Model	SDE	Stocks	Energy
Disc.	TSGM	VP subVP	.022±.005 .021±.008	.221±.025 .198±.025
	w/o pre-training	VP subVP	.022±.004 .059±.006	.322±.003 .284±.004
Pred.	TSGM	VP subVP	.037±.000 .037±.000	.257±.000 .252±.000
	w/o pre-training	VP subVP	.037±.000 .037±.000	.252±.000 .251±.000

Table 4: Comparison between with and without pre-training the autoencoder. For other omitted datasets, we can observe similar patterns.

recall from the original data. Therefore, TSGM generates diverse synthetic samples in comparison with TimeGAN and TimeVAE in all cases. Especially, TSGM achieves much higher diversity than the two models on Energy and Air.

Ablation and Sensitivity Studies

Ablation study As an ablation study, we simultaneously train the conditional score network, encoder, and decoder from scratch. The results are in Table 4. There ablation models are worse than the full model, but they still outperform many baselines.

Sensitivity study We conduct two sensitivity studies: i) reducing the depth of U-net, ii) decreasing the sampling step numbers. The results are in Table 5.

At first, we modify the depth of U-net from 4 to 3 to check the performance of the lighter conditional score network. Surprisingly, we achieve a better discriminative score with a

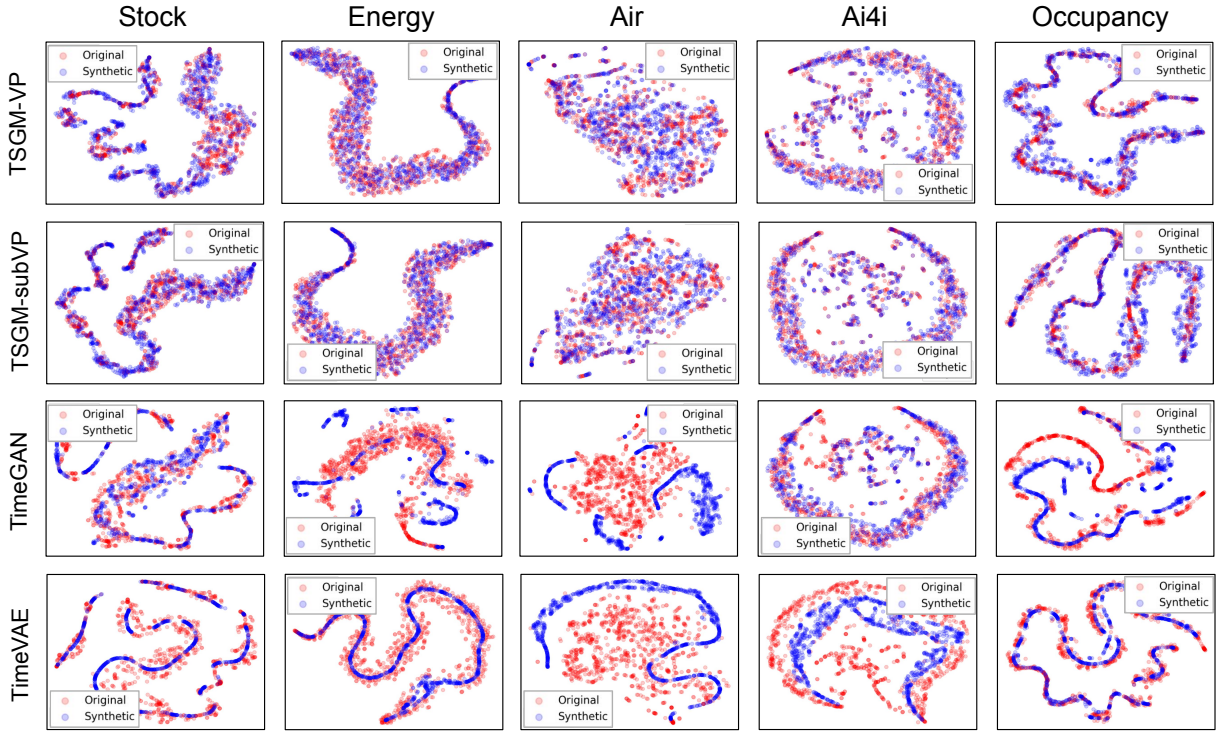


Figure 2: t-SNE plots for TSGM (1st and 2nd rows), TimeGAN (3rd row), and TimeVAE (4th row). Red and blue dots mean original and synthesized samples, respectively.

slight loss on the predictive score.

Next, we decrease the number of sampling steps for faster sampling from 1000 steps to 500, 250, and 100 steps, respectively. For VP, we achieve almost the same results with 500 steps. Surprisingly, in the case of subVP, we achieve good results until 100 steps.

Empirical Complexity Analyses

We also report the memory footprint and runtime for sampling fake data in Appendix for space reasons. In general, our method requires a longer sampling time than TimeGAN and some other simple methods.

Conclusion & Limitations

We presented a score-based generative model framework for time-series generation. We combined an RNN-based autoencoder and our score network into a single framework to accomplish the goal. We also designed an appropriate denoising score matching loss for our generation task and achieved the state-of-the-art results on various datasets in terms of the discriminative and predictive scores. In addition, we conducted rigorous ablation and sensitivity studies to prove the efficacy of our model design.

Although our method achieves the state-of-the-art sampling quality and diversity, there exists a fundamental problem that all SGMs have. That is, SGMs are slower than GANs for generating samples. Since there are several accomplishments for faster sampling (Xiao, Kreis, and Vahdat 2022; Jolicoeur-Martineau et al. 2021), however, one can apply

them to our method and it would be much faster without any loss of sampling quality and diversity. One can also use other types of autoencoders instead of our RNN-based one. For instance, other continuous-time autoencoder methods are known to be able to process irregular time-series (Rubanova, Chen, and Duvenaud 2019). Our proposed score-based methods are naturally benefited by using those advanced autoencoders. In addition, we did not search miscellaneous hyperparameters by reusing the default values in TimeGAN (Yoon, Jarrett, and van der Schaar 2019) and VPSDE (Song et al. 2021), which means there still exists room to improve.

References

- Ahmed, N. K.; Atiya, A. F.; Gayar, N. E.; and El-Shishiny, H. 2010. An Empirical Comparison of Machine Learning Models for Time Series Forecasting. *Econometric Reviews*, 29(5-6): 594–621.
- Anderson, B. D. 1982. Reverse-time diffusion equation models. *Stochastic Processes and their Applications*, 12(3): 313–326.
- Candanedo, L. M.; Feldheim, V.; and Deramaix, D. 2017. Data driven prediction models of energy use of appliances in a low-energy house. *Energy and Buildings*, 140: 81–97.
- Chu, C.; Minami, K.; and Fukumizu, K. 2020. Smoothness and Stability in GANs. In *International Conference on Learning Representations*.
- De Vito, S.; Massera, E.; Piga, M.; Martinotto, L.; and Di Francia, G. 2008. On field calibration of an electronic nose

	Model	SDE	Stocks	Energy
Disc.	TSGM	VP	.022±.005	.221±.025
		subVP	.021±.008	.198±.025
	depth of 3	VP	.022±.004	.175±.009
		subVP	.020±.007	.182±.009
	500 steps	VP	.025±.005	.259±.003
		subVP	.020±.004	.248±.002
	250 steps	VP	.067±.009	.250±.003
		subVP	.022±.009	.247±.002
	100 steps	VP	.202±.013	.325±.003
		subVP	.023±.005	.237±.004
Pred.	TSGM	VP	.037±.000	.257±.000
		subVP	.037±.000	.252±.000
	depth of 3	VP	.037±.000	.253±.000
		subVP	.037±.000	.253±.000
	500 steps	VP	.037±.000	.257±.000
		subVP	.037±.000	.253±.000
	250 steps	VP	.037±.000	.256±.000
		subVP	.037±.000	.253±.000
	100 steps	VP	.039±.000	.256±.000
		subVP	.037±.000	.253±.000

Table 5: Sensitivity results on the depth of U-net and the number of sampling steps

for benzene estimation in an urban pollution monitoring scenario. *Sensors and Actuators B: Chemical*, 129(2): 750–757.

Desai, A.; Freeman, C.; Wang, Z.; and Beaver, I. 2021. TimeVAE: A Variational Auto-Encoder for Multivariate Time Series Generation. *arXiv:2111.08095*.

Donahue, C.; McAuley, J.; and Puckette, M. 2019. Adversarial audio synthesis. In *International Conference on Learning Representations*.

Esteban, C.; Hyland, S. L.; and Rätsch, G. 2017. Real-valued (Medical) Time Series Generation with Recurrent Conditional GANs. *arXiv:1706.02633*.

Fu, T. 2011. A review on time series data mining. *Engineering Applications of Artificial Intelligence*, 24(1): 164–181.

Goyal, A.; Lamb, A.; Zhang, Y.; Zhang, S.; Courville, A.; and Bengio, Y. 2016. Professor Forcing: A New Algorithm for Training Recurrent Networks. In *Advances in Neural Information Processing Systems*.

Graves, A. 2013. Generating Sequences With Recurrent Neural Networks. *arXiv:1308.0850*.

Ho, J.; Jain, A.; and Abbeel, P. 2020. Denoising diffusion probabilistic models. In *Advances in Neural Information Processing Systems*.

Ismail Fawaz, H.; Forestier, G.; Weber, J.; Idoumghar, L.; and Muller, P.-A. 2019. Deep learning for time series classification: a review. *Data Mining and Knowledge Discovery*, 33: 917–963.

Jolicœur-Martineau, A.; Li, K.; Piché-Taillefer, R.; Kachman, T.; and Mitliagkas, I. 2021. Gotta Go Fast When Generating Data with Score-Based Models. *CoRR*, abs/2105.14080.

Karras, T.; Laine, S.; Aittala, M.; Hellsten, J.; Lehtinen, J.; and Aila, T. 2019. Analyzing and Improving the Image Quality of StyleGAN. *CoRR*, abs/1912.04958.

Kim, J.; Lee, C.; Shin, Y.; Park, S.; Kim, M.; Park, N.; and Cho, J. 2022. SOS: Score-based Oversampling for Tabular Data. In *Proceedings of the 28th ACM SIGKDD Conference on Knowledge Discovery and Data Mining*.

Matzka, S. 2020. AI4I 2020 Predictive Maintenance Dataset. <https://archive.ics.uci.edu/ml/datasets/AI4I+2020+Predictive+Maintenance+Dataset>.

Mittal, G.; Engel, J. H.; Hawthorne, C.; and Simon, I. 2021. Symbolic Music Generation with Diffusion Models. *CoRR*, abs/2103.16091.

Mogren, O. 2016. C-RNN-GAN: A continuous recurrent neural network with adversarial training. In *Constructive Machine Learning Workshop (CML) at NeurIPS 2016*.

Rasul, K.; Seward, C.; Schuster, I.; and Vollgraf, R. 2021. Autoregressive Denoising Diffusion Models for Multivariate Probabilistic Time Series Forecasting. In *International Conference on Machine Learning*.

Ronneberger, O.; Fischer, P.; and Brox, T. 2015. U-Net: Convolutional Networks for Biomedical Image Segmentation. In *Medical Image Computing and Computer-Assisted Intervention (MICCAI)*, 234–241.

Rubanova, Y.; Chen, R. T. Q.; and Duvenaud, D. K. 2019. Latent Ordinary Differential Equations for Irregularly-Sampled Time Series. In *NeurIPS*.

Sohl-Dickstein, J.; Weiss, E.; Maheswaranathan, N.; and Ganguli, S. 2015. Deep unsupervised learning using nonequilibrium thermodynamics. In *International Conference on Machine Learning*.

Song, Y.; and Ermon, S. 2019. Generative modeling by estimating gradients of the data distribution. In *Advances in Neural Information Processing Systems*.

Song, Y.; Shen, L.; Xing, L.; and Ermon, S. 2022. Solving Inverse Problems in Medical Imaging with Score-Based Generative Models. In *International Conference on Learning Representations*.

Song, Y.; Sohl-Dickstein, J.; Kingma, D. P.; Kumar, A.; Ermon, S.; and Poole, B. 2021. Score-Based Generative Modeling through Stochastic Differential Equations. In *International Conference on Learning Representations*.

Sutskever, I.; Martens, J.; and Hinton, G. 2011. Generating Text with Recurrent Neural Networks. In *Proceedings of the 28th International Conference on International Conference on Machine Learning*, 1017–1024.

Särkkä, S.; and Solin, A., eds. 2019. *Applied stochastic differential equations*, volume 10. Cambridge University Press.

Tashiro, Y.; Song, J.; Song, Y.; and Ermon, S. 2021. CSDI: Conditional Score-based Diffusion Models for Probabilistic Time Series Imputation. In *Advances in Neural Information Processing Systems*.

van der Maaten, L.; and Hinton, G. 2008. Visualizing data using t-SNE. *Journal of machine learning research*, 9(86): 2579–2605.

Vincent, P. 2011. A Connection Between Score Matching and Denoising Autoencoders. *Neural Computation*, 23(7): 1661–1674.

- Xiao, Z.; Kreis, K.; and Vahdat, A. 2022. Tackling the Generative Learning Trilemma with Denoising Diffusion GANs. In *International Conference on Learning Representations*.
- Xu, T.; Wenliang, L. K.; Munn, M.; and Acciaio, B. 2020. COT-GAN: Generating Sequential Data via Causal Optimal Transport. In *Advances in Neural Information Processing Systems*.
- Yan, T.; Zhang, H.; Zhou, T.; Zhan, Y.; and Xia, Y. 2021. ScoreGrad: Multivariate Probabilistic Time Series Forecasting with Continuous Energy-based Generative Models. *arXiv:2106.10121*.
- Yoon, J.; Jarrett, D.; and van der Schaar, M. 2019. Time-series Generative Adversarial Networks. In *Advances in Neural Information Processing Systems*.

TSGM: Time-series Generation using Score-based Generative Models

– Supplementary Material –

A Proofs

Theorem 2 (Denoising score matching on time-series). $l_1(t, s)$ can be replaced by the following $l_2(t, s)$:

$$l_2(t, s) = \mathbb{E}_{\mathbf{x}_t} \mathbb{E}_{\mathbf{x}_{1:t}^s} \left[\left\| M_\theta(s, \mathbf{x}_{1:t}^s, \mathbf{x}_{1:t-1}) - \nabla_{\mathbf{x}_{1:t}^s} \log p(\mathbf{x}_{1:t}^s | \mathbf{x}_{1:t-1}) \right\|_2^2 \right],$$

where \mathbf{x}_t and $\mathbf{x}_{1:t}^s$ are sampled from $p(\mathbf{x}_t | \mathbf{x}_{1:t-1})$ and $p(\mathbf{x}_{1:t}^s | \mathbf{x}_{1:t-1})$. Therefore, we can use an alternative objective,

$$L_2 = \mathbb{E}_s \mathbb{E}_{\mathbf{x}_{1:T}} \left[\sum_{t=1}^T \lambda(s) l_2(t, s) \right] \text{ instead of } L_1$$

proof. At first, if $t = 1$, it can be substituted with the naive denoising score loss by (Vincent 2011) since $\mathbf{x}_0 = \mathbf{0}$.

Next, let us consider $t > 1$. $l_1(t, s)$ can be decomposed as follows:

$$l_1(t, s) = -2 \cdot \mathbb{E}_{\mathbf{x}_{1:t}^s} \langle M_\theta(s, \mathbf{x}_{1:t}^s, \mathbf{x}_{1:t-1}), \nabla_{\mathbf{x}_{1:t}^s} \log p(\mathbf{x}_{1:t}^s | \mathbf{x}_{1:t-1}) \rangle + \mathbb{E}_{\mathbf{x}_{1:t}^s} \left[\left\| M_\theta(s, \mathbf{x}_{1:t}^s, \mathbf{x}_{1:t-1}) \right\|_2^2 \right] + C_1$$

Here, C_1 is a constant that does not depend on the parameter θ , and $\langle \cdot, \cdot \rangle$ mean the inner product. Then, the first part's expectation of the right-hand side can be expressed as follows:

$$\begin{aligned} & \mathbb{E}_{\mathbf{x}_{1:t}^s} [\langle M_\theta(s, \mathbf{x}_{1:t}^s, \mathbf{x}_{1:t-1}), \nabla_{\mathbf{x}_{1:t}^s} \log p(\mathbf{x}_{1:t}^s | \mathbf{x}_{1:t-1}) \rangle] \\ &= \int_{\mathbf{x}_{1:t}^s} \langle M_\theta(s, \mathbf{x}_{1:t}^s, \mathbf{x}_{1:t-1}), \nabla_{\mathbf{x}_{1:t}^s} \log p(\mathbf{x}_{1:t}^s | \mathbf{x}_{1:t-1}) \rangle p(\mathbf{x}_{1:t}^s | \mathbf{x}_{1:t-1}) d\mathbf{x}_{1:t}^s \\ &= \int_{\mathbf{x}_{1:t}^s} \langle M_\theta(s, \mathbf{x}_{1:t}^s, \mathbf{x}_{1:t-1}), \frac{1}{p(\mathbf{x}_{1:t-1})} \frac{\partial p(\mathbf{x}_{1:t}^s, \mathbf{x}_{1:t-1})}{\partial \mathbf{x}_{1:t}^s} \rangle d\mathbf{x}_{1:t}^s \\ &= \int_{\mathbf{x}_t} \int_{\mathbf{x}_{1:t}^s} \langle M_\theta(s, \mathbf{x}_{1:t}^s, \mathbf{x}_{1:t-1}), \frac{1}{p(\mathbf{x}_{1:t-1})} \frac{\partial p(\mathbf{x}_{1:t}^s, \mathbf{x}_{1:t-1}, \mathbf{x}_t)}{\partial \mathbf{x}_{1:t}^s} \rangle d\mathbf{x}_{1:t}^s d\mathbf{x}_t \\ &= \int_{\mathbf{x}_t} \int_{\mathbf{x}_{1:t}^s} \langle M_\theta(s, \mathbf{x}_{1:t}^s, \mathbf{x}_{1:t-1}), \frac{\partial p(\mathbf{x}_{1:t}^s | \mathbf{x}_{1:t})}{\partial \mathbf{x}_{1:t}^s} \rangle \frac{p(\mathbf{x}_{1:t-1}, \mathbf{x}_t)}{p(\mathbf{x}_{1:t-1})} d\mathbf{x}_{1:t}^s d\mathbf{x}_t \\ &= \int_{\mathbf{x}_t} \int_{\mathbf{x}_{1:t}^s} \langle M_\theta(s, \mathbf{x}_{1:t}^s, \mathbf{x}_{1:t-1}), \frac{\partial p(\mathbf{x}_{1:t}^s | \mathbf{x}_{1:t})}{\partial \mathbf{x}_{1:t}^s} \rangle p(\mathbf{x}_t | \mathbf{x}_{1:t-1}) d\mathbf{x}_{1:t}^s d\mathbf{x}_t \\ &= \mathbb{E}_{\mathbf{x}_t} \left[\int_{\mathbf{x}_{1:t}^s} \langle M_\theta(s, \mathbf{x}_{1:t}^s, \mathbf{x}_{1:t-1}), \frac{\partial p(\mathbf{x}_{1:t}^s | \mathbf{x}_{1:t})}{\partial \mathbf{x}_{1:t}^s} \rangle d\mathbf{x}_{1:t}^s \right] \\ &= \mathbb{E}_{\mathbf{x}_t} \left[\int_{\mathbf{x}_{1:t}^s} \langle M_\theta(s, \mathbf{x}_{1:t}^s, \mathbf{x}_{1:t-1}), \nabla_{\mathbf{x}_{1:t}^s} \log p(\mathbf{x}_{1:t}^s | \mathbf{x}_{1:t}) \rangle p(\mathbf{x}_{1:t}^s | \mathbf{x}_{1:t}) d\mathbf{x}_{1:t}^s \right] \\ &= \mathbb{E}_{\mathbf{x}_t} \mathbb{E}_{\mathbf{x}_{1:t}^s} [\langle M_\theta(s, \mathbf{x}_{1:t}^s, \mathbf{x}_{1:t-1}), \nabla_{\mathbf{x}_{1:t}^s} \log p(\mathbf{x}_{1:t}^s | \mathbf{x}_{1:t}) \rangle] \end{aligned}$$

Similarly, the second part's expectation of the right-hand side can be rewritten as follows:

$$\begin{aligned} & \mathbb{E}_{\mathbf{x}_{1:t}^s} [\left\| M_\theta(s, \mathbf{x}_{1:t}^s, \mathbf{x}_{1:t-1}) \right\|_2^2] \\ &= \int_{\mathbf{x}_{1:t}^s} \left\| M_\theta(s, \mathbf{x}_{1:t}^s, \mathbf{x}_{1:t-1}) \right\|_2^2 \cdot p(\mathbf{x}_{1:t}^s | \mathbf{x}_{1:t-1}) d\mathbf{x}_{1:t}^s \\ &= \int_{\mathbf{x}_t} \int_{\mathbf{x}_{1:t}^s} \left\| M_\theta(s, \mathbf{x}_{1:t}^s, \mathbf{x}_{1:t-1}) \right\|_2^2 \cdot \frac{p(\mathbf{x}_{1:t}^s, \mathbf{x}_{1:t-1}, \mathbf{x}_t)}{p(\mathbf{x}_{1:t-1})} d\mathbf{x}_{1:t}^s d\mathbf{x}_t \\ &= \int_{\mathbf{x}_t} \int_{\mathbf{x}_{1:t}^s} \left\| M_\theta(s, \mathbf{x}_{1:t}^s, \mathbf{x}_{1:t-1}) \right\|_2^2 \cdot p(\mathbf{x}_{1:t}^s | \mathbf{x}_{1:t}) \frac{p(\mathbf{x}_{1:t-1}, \mathbf{x}_t)}{p(\mathbf{x}_{1:t-1})} d\mathbf{x}_{1:t}^s d\mathbf{x}_t \\ &= \int_{\mathbf{x}_t} \int_{\mathbf{x}_{1:t}^s} \left\| M_\theta(s, \mathbf{x}_{1:t}^s, \mathbf{x}_{1:t-1}) \right\|_2^2 \cdot p(\mathbf{x}_{1:t}^s | \mathbf{x}_{1:t}) p(\mathbf{x}_t | \mathbf{x}_{1:t-1}) d\mathbf{x}_{1:t}^s d\mathbf{x}_t \\ &= \mathbb{E}_{\mathbf{x}_t} \mathbb{E}_{\mathbf{x}_{1:t}^s} [\left\| M_\theta(s, \mathbf{x}_{1:t}^s, \mathbf{x}_{1:t-1}) \right\|_2^2] \end{aligned}$$

Finally, by using above results, we can derive following result:

$$\begin{aligned} l_1 &= \mathbb{E}_{\mathbf{x}_t} \mathbb{E}_{\mathbf{x}_{1:t}^s} \left[\left\| M_\theta(s, \mathbf{x}_{1:t}^s, \mathbf{x}_{1:t-1}) \right\|_2^2 \right] + C_1 \\ &\quad - 2 \cdot \mathbb{E}_{\mathbf{x}_t} \mathbb{E}_{\mathbf{x}_{1:t}^s} \langle M_\theta(s, \mathbf{x}_{1:t}^s, \mathbf{x}_{1:t-1}), \nabla_{\mathbf{x}_{1:t}^s} \log p(\mathbf{x}_{1:t}^s | \mathbf{x}_{1:t-1}) \rangle \\ &= \mathbb{E}_{\mathbf{x}_t} \mathbb{E}_{\mathbf{x}_{1:t}^s} \left[\left\| M_\theta(s, \mathbf{x}_{1:t}^s, \mathbf{x}_{1:t-1}) - \nabla_{\mathbf{x}_{1:t}^s} \log p(\mathbf{x}_{1:t}^s | \mathbf{x}_{1:t-1}) \right\|_2^2 \right] + C \end{aligned}$$

C is a constant that does not depend on the parameter θ . \square

Corollary 2. Our target objective function, L_{score} , is defined as follows:

$$L_{score} = \mathbb{E}_s \mathbb{E}_{\mathbf{x}_{1:T}} \left[\sum_{t=1}^T \lambda(s) l_2^*(t, s) \right],$$

where

$$l_2^*(t, s) = \mathbb{E}_{\mathbf{x}_{1:t}^s} \left[\left\| M_\theta(s, \mathbf{x}_{1:t}^s, \mathbf{x}_{1:t-1}) - \nabla_{\mathbf{x}_{1:t}^s} \log p(\mathbf{x}_{1:t}^s | \mathbf{x}_{1:t-1}) \right\|_2^2 \right].$$

Then, $L_2 = L_{score}$ is satisfied.

proof. Whereas one can use the law of total expectation, which means $E[X] = E[E[X|Y]]$ if X, Y are on an identical probability space to show the above formula, we calculate directly. At first, let us simplify the expectation of the inner part with a symbol $f(\mathbf{x}_{1:t})$ for our computational convenience, i.e., $f(\mathbf{x}_{1:t}) = \mathbb{E}_s \mathbb{E}_{\mathbf{x}_{1:t}^s} \left[\lambda(s) \left\| M_\theta(s, \mathbf{x}_{1:t}^s, \mathbf{x}_{1:t-1}) - \nabla_{\mathbf{x}_{1:t}^s} \log p(\mathbf{x}_{1:t}^s | \mathbf{x}_{1:t-1}) \right\|_2^2 \right]$. Then we have the following definition:

$$L_2 = \mathbb{E}_s \mathbb{E}_{\mathbf{x}_{1:T}} [l_2] = \mathbb{E}_{\mathbf{x}_{1:T}} \left[\sum_{t=1}^T \mathbb{E}_{\mathbf{x}_t} [f(\mathbf{x}_{1:t})] \right] = \sum_{t=1}^T \mathbb{E}_{\mathbf{x}_{1:T}} \mathbb{E}_{\mathbf{x}_t} [f(\mathbf{x}_{1:t})]$$

At last, the expectation part can be further simplified as follows:

$$\begin{aligned} & \mathbb{E}_{\mathbf{x}_{1:T}} \mathbb{E}_{\mathbf{x}_t} [f(\mathbf{x}_{1:t})] \\ &= \int_{\mathbf{x}_{1:T}} \int_{\mathbf{x}_t} f(\mathbf{x}_{1:t}) p(\mathbf{x}_t | \mathbf{x}_{1:t-1}) d\mathbf{x}_t \cdot p(\mathbf{x}_{1:t-1}) p(\mathbf{x}_{t:T} | \mathbf{x}_{1:t-1}) d\mathbf{x}_{1:T} \\ &= \int_{\mathbf{x}_{1:T}} \int_{\mathbf{x}_t} f(\mathbf{x}_{1:t}) p(\mathbf{x}_{1:t}) d\mathbf{x}_t \cdot p(\mathbf{x}_{t:T} | \mathbf{x}_{1:t-1}) d\mathbf{x}_{1:T} \\ &= \int_{\mathbf{x}_{t:T}} \left(\int_{\mathbf{x}_{1:t}} f(\mathbf{x}_{1:t}) p(\mathbf{x}_{1:t}) d\mathbf{x}_{1:t} \right) p(\mathbf{x}_{t:T} | \mathbf{x}_{1:t-1}) d\mathbf{x}_{t:T} \\ &= \int_{\mathbf{x}_{1:t}} f(\mathbf{x}_{1:t}) p(\mathbf{x}_{1:t}) d\mathbf{x}_{1:t} \\ &= \int_{\mathbf{x}_{1:t}} \left(\int_{\mathbf{x}_{t+1:T}} p(\mathbf{x}_{t+1:T} | \mathbf{x}_{1:t}) d\mathbf{x}_{t+1:T} \right) f(\mathbf{x}_{1:t}) p(\mathbf{x}_{1:t}) d\mathbf{x}_{1:t} \\ &= \int_{\mathbf{x}_{1:T}} f(\mathbf{x}_{1:t}) p(\mathbf{x}_{1:T}) d\mathbf{x}_{1:T} \\ &= \mathbb{E}_{\mathbf{x}_{1:T}} [f(\mathbf{x}_{1:t})] \end{aligned}$$

Since $\sum_{t=1}^T \mathbb{E}_{\mathbf{x}_{1:T}} [f(\mathbf{x}_{1:t})] = \mathbb{E}_{\mathbf{x}_{1:T}} [\sum_{t=1}^T f(\mathbf{x}_{1:t})] = L_{score}$, we prove the corollary. \square

B Datasets and Baselines

We use 5 datasets from various fields as follows. We summarize their data dimensions, the number of training samples, and their time-series lengths (window sizes) in Table A.

- *Stock* (Yoon, Jarrett, and van der Schaar 2019): The Google stock dataset was collected irregularly from 2004 to 2019. Each observation has (volume, high, low, opening, closing, adjusted closing prices), and these features are correlated.
- *Energy* (Candanedo, Feldheim, and Deramaix 2017): This dataset is from the UCI machine learning repository for predicting the energy use of appliances from highly correlated variables such as house temperature and humidity conditions.
- *Air* (De Vito et al. 2008): The UCI Air Quality dataset were collected from 2004 to 2005. Hourly averaged air quality records are gathered using gas sensor devices in an Italian city.
- *AI4I* (Matzka 2020): AI4I means the UCI AI4I 2020 Predictive Maintenance dataset. This data reflects the industrial predictive maintenance scenario with correlated features including several physical quantities.
- *Occupancy* (Candanedo and Feldheim 2016): The UCI Room Occupancy Estimation dataset contains features such as temperature, light, and CO2 collected from multiple environmental sensors.

We use several types of generative methods for time-series as baselines. At first, we consider autoregressive generative methods: T-Forcing (teacher forcing) (Graves 2013; Sutskever, Martens, and Hinton 2011) and P-Forcing (professor forcing) (Goyal et al. 2016). Next, we use GAN-based methods: TimeGAN (Yoon, Jarrett, and van der Schaar 2019), RCGAN (Esteban, Hyland, and Rätsch 2017), C-RNN-GAN (Mogren 2016), COT-GAN (Xu et al. 2020), WaveGAN (Donahue, McAuley, and Puckette 2019). Finally, we also test VAE-based methods into our baselines: TimeVAE (Desai et al. 2021).

Dataset	Dimension	#Samples	Length
Stocks	6	3685	24
Energy	28	19735	
Air	13	9357	
AI4I	5	10000	
Occupancy	13	10129	

Table A: Characteristics of the datasets we use for our experiments

C Search Space for Hyperparameters

We give our search space for hyperparameters. $iter_{pre}$, is in $\{50000, 100000\}$. The dimension of hidden features, d_{hidden} , ranges from 2 times to 5 times the dimension of input features. For other settings, we follow the default values in TimeGAN (Yoon, Jarrett, and van der Schaar 2019) and VPSDE (Song et al. 2021).

D Miscellaneous Experimental Environments

We give detailed experimental environments. The following software and hardware environments were used for all experiments: UBUNTU 18.04 LTS, PYTHON 3.9.12, CUDA 9.1, and NVIDIA Driver 470.141, and i9 CPU, and GEFORCE RTX 2080 Ti.

On the experiments, We report only the VP and subVP-based TSGM and exclude the VE-based one for its lower performance. For baselines, we reuse their released source codes in their official repositories and rely on their designed training and model selection procedures. For our method, we select the best model every 5000 iteration. For this, we synthesize samples, and calculate the mean and standard deviation scores of the discriminative and predictive scores.

E Empirical Space and Time Complexity Analyses

We report the memory usage during training in Table B and the wall-clock time for generating 1,000 time-series samples in Table C. We compare only with TimeGAN (Yoon, Jarrett, and van der Schaar 2019) since is the state-of-the-art method. Our method is relatively slower than TimeGAN, which is a fundamental drawback of all SGMs. For example, the original score-based model (Song et al. 2021) requires 3,214 seconds for sampling 1,000 CIFAR-10 images while StyleGAN (Karras et al. 2019) needs 0.4 seconds. However, we also emphasize that this problem can be relieved by using the techniques suggested in (Xiao, Kreis, and Vahdat 2022; Jolicoeur-Martineau et al. 2021) as we mentioned in the conclusion section.

Model	Stock	Energy
TimeGAN	1.1(GB)	1.6(GB)
TSGM	3.8(GB)	3.9(GB)

Table B: The memory usage for training

Model	Stocks	Energy
TSGM	3318.99(s)	1620.84(s)
TimeGAN	0.43(s)	0.47(s)

Table C: The sampling time of TSGM and TimeGAN for generating 1,000 samples on each dataset. The original score-based model (Song et al. 2021) requires 3,214 seconds for sampling 1000 CIFAR-10 images while StyleGAN (Karras et al. 2019) needs 0.4 seconds, which is a similar ratio to our results.

References

- Candanedo, L. M.; and Feldheim, V. 2016. Accurate occupancy detection of an office room from light, temperature, humidity and CO2 measurements using statistical learning models. *Energy and Buildings*, 112: 28–39.
- Candanedo, L. M.; Feldheim, V.; and Deramaix, D. 2017. Data driven prediction models of energy use of appliances in a low-energy house. *Energy and Buildings*, 140: 81–97.

De Vito, S.; Massera, E.; Piga, M.; Martinotto, L.; and Di Francia, G. 2008. On field calibration of an electronic nose for benzene estimation in an urban pollution monitoring scenario. *Sensors and Actuators B: Chemical*, 129(2): 750–757.

Desai, A.; Freeman, C.; Wang, Z.; and Beaver, I. 2021. TimeVAE: A Variational Auto-Encoder for Multivariate Time Series Generation. *arXiv:2111.08095*.

Donahue, C.; McAuley, J.; and Puckette, M. 2019. Adversarial audio synthesis. In *International Conference on Learning Representations*.

Esteban, C.; Hyland, S. L.; and Rätsch, G. 2017. Real-valued (Medical) Time Series Generation with Recurrent Conditional GANs. *arXiv:1706.02633*.

Goyal, A.; Lamb, A.; Zhang, Y.; Zhang, S.; Courville, A.; and Bengio, Y. 2016. Professor Forcing: A New Algorithm for Training Recurrent Networks. In *Advances in Neural Information Processing Systems*.

Graves, A. 2013. Generating Sequences With Recurrent Neural Networks. *arXiv:1308.0850*.

Jolicoeur-Martineau, A.; Li, K.; Piché-Taillefer, R.; Kachman, T.; and Mitliagkas, I. 2021. Gotta Go Fast When Generating Data with Score-Based Models. *CoRR*, abs/2105.14080.

Karras, T.; Laine, S.; Aittala, M.; Hellsten, J.; Lehtinen, J.; and Aila, T. 2019. Analyzing and Improving the Image Quality of StyleGAN. *CoRR*, abs/1912.04958.

Matzka, S. 2020. AI4I 2020 Predictive Maintenance Dataset. <https://archive.ics.uci.edu/ml/datasets/AI4I+2020+Predictive+Maintenance+Dataset>.

Mogren, O. 2016. C-RNN-GAN: A continuous recurrent neural network with adversarial training. In *Constructive Machine Learning Workshop (CML) at NeurIPS 2016*.

Song, Y.; Sohl-Dickstein, J.; Kingma, D. P.; Kumar, A.; Ermon, S.; and Poole, B. 2021. Score-Based Generative Modeling through Stochastic Differential Equations. In *International Conference on Learning Representations*.

Sutskever, I.; Martens, J.; and Hinton, G. 2011. Generating Text with Recurrent Neural Networks. In *Proceedings of the 28th International Conference on International Conference on Machine Learning*, 1017–1024.

Vincent, P. 2011. A Connection Between Score Matching and Denoising Autoencoders. *Neural Computation*, 23(7): 1661–1674.

Xiao, Z.; Kreis, K.; and Vahdat, A. 2022. Tackling the Generative Learning Trilemma with Denoising Diffusion GANs. In *International Conference on Learning Representations*.

Xu, T.; Wenliang, L. K.; Munn, M.; and Acciaio, B. 2020. COT-GAN: Generating Sequential Data via Causal Optimal Transport. In *Advances in Neural Information Processing Systems*.

Yoon, J.; Jarrett, D.; and van der Schaar, M. 2019. Time-series Generative Adversarial Networks. In *Advances in Neural Information Processing Systems*.